

Universal properties of Dark Matter halos

A. Boyarsky,^{1,2} A. Neronov,³ O. Ruchayskiy,¹ and I. Tkachev⁴

¹*Ecole Polytechnique Fédérale de Lausanne, FSB/ITP/LPPC, BSP 720, CH-1015, Lausanne, Switzerland*

²*Bogolyubov Institute of Theoretical Physics, Kyiv, Ukraine*

³*INTEGRAL Science Data Center, Versoix and Geneva Observatory, Sauverny, Switzerland*

⁴*Institute for Nuclear Researches, Moscow, Russia*

(■Dated: November 17, 2009)

We discuss the universal relation between density and size of observed Dark Matter halos that was recently shown to hold on a wide range of scales, from dwarf galaxies to galaxy clusters. Predictions of Λ CDM N-body simulations are consistent with this relation. We demonstrate that this property of Λ CDM can be understood analytically in the secondary infall model. Qualitative understanding given by this model provides a new way to predict which deviations from Λ CDM or large-scale modifications of gravity can affect universal behavior and, therefore, to constrain them observationally.

PACS numbers: 95.35.+d, 98.62.Gq

Introduction. The nature of Dark Matter (DM) is one of the most fundamental puzzles in modern physics (see e.g. [1] for a recent review). Resolution of this puzzle may potentially shed a light on many fundamental physical issues, including particle physics beyond the Standard Model, large-scale properties of gravity, etc. The simplest Cold Dark Matter (CDM) model is rather successful in explaining cosmological and astronomical observational data at large distances [2]. More complicated models, discussed in the literature, include “warm” DM models [3], or models with modifications of large-scale properties of gravity [4] or even of Newtonian dynamics [5]. Search for deviations from the CDM predictions provides an important tool to constrain the properties of unknown DM particles and to test fundamental laws of gravity.

Comparison of predictions of DM models with observational data is complicated by the fact that information about the properties of DM halos is usually derived from the study of dynamics of “luminous tracers”: stars and gas particles (the only exception being gravitational lensing method). Physics of the luminous baryonic matter in galaxies and galaxy clusters is very nontrivial to be fully accounted for in theoretical and numerical modeling. Thus, it is crucial to find the properties of DM distributions that do not depend on the physics of the baryonic matter and, therefore, could be directly compared with predictions of pure DM models. Below, we argue that recently discovered relation between characteristic density and size of the DM halos of galaxies and galaxy clusters may provide an example of such a “universal” relation, and suggest its analytical understanding within the CDM model.

Universal properties of DM halos. It was discussed for a long time (see [6–8] and references therein) that sizes and densities of observed galactic DM halos obey a universal scaling relation. Namely, the DM central density $\bar{\rho}_C$, averaged over a region with the characteristic size r_C of the halo, scales roughly as r_C^{-1} . This scaling law might appear surprising, if one takes into account quite different histories of formation of various galaxies and their different types. No clear qualitative understanding of the origin of “dilution” of the density of DM halos with the increase of the halo size was proposed so far.

A different scaling relation between parameters of DM distribution was suggested in [9] for still larger range of distance and mass scales. The authors of [9] collected published data on the DM distributions in 289 objects ranging from dwarf spheroidal galaxies (dSphs) to galaxy clusters. The observational data were fit by different density profiles: Navarro-Frenk-White (NFW) [10], (pseudo)-isothermal (ISO), Burkert (BURK) [11] and on average 3 density profiles were collected for each object. It was found that the average “column density” of DM halos

$$\mathcal{S} = \frac{2}{r_C^2} \int_0^{r_C} r' dr' \int_{-\infty}^{\infty} dz \rho(\sqrt{r'^2 + z^2}) \quad (1)$$

slowly grows with the increase of the mass of the halo as

$$\mathcal{S} \simeq 61 \left[\frac{M_{200}}{10^{10} M_\odot} \right]^{0.21} \frac{M_\odot}{\text{pc}^2} \quad (2)$$

where M_{200} is the measure of the halo mass (it is the mass contained within a sphere of the radius R_{200} where the average DM density equals to $200\rho_{\text{crit}}$ with ρ_{crit} being the critical density of the Universe today). The parameter r_C in (1) is taken to be r_s of the NFW profile that fits the observed DM distribution. If the same data (e.g. rotation curves in galaxies or temperature profiles of galaxy clusters) were fitted using a different DM profile, the scale r_C may be uniquely expressed in terms of the parameters of that profile. The column density (1) is insensitive to the type of DM density profile used to fit the same observational data (see [9] for details).

From Eq. (1) it follows that $\mathcal{S} \propto \bar{\rho}_C r_C$. Therefore, for cored profiles (ISO or BURK) the relation (2) is a generalization of the previously considered relation $\bar{\rho}_C r_C \simeq \text{const}$ [6, 7]. However, the quantity \mathcal{S} is more universal, as it is defined for any (not necessarily cored) DM profile. Therefore, in [9] \mathcal{S} was derived for *any* type of DM density profile, used by observers to describe the DM distribution in halos in the broad range of sizes ($0.2 \text{ kpc} \lesssim r_C \lesssim 2.5 \text{ Mpc}$) and masses ($10^8 M_\odot < M_{200} < 10^{16} M_\odot$). The relation $\bar{\rho}_C r_C \simeq 141 M_\odot \text{ pc}^{-2}$, derived in [7] for galaxies, and $\mathcal{S} \sim 200 M_\odot \text{ pc}^{-2}$, proposed in

the Ref. [12] for galaxies and galaxy clusters, could serve as approximations of relation (2) at low- and high-mass ends of the data. This is clear from Fig. 1 in which the data from [9] are presented together with the fit (2) (solid line).

The relation (2) is derived from the analysis of data on DM halos of structures with significantly different physics of the luminous matter. (from stars in dwarf galaxies through gaseous disks at the outskirts of spiral galaxies to hot intra-cluster medium gas in galaxy clusters). The fact that the properties of DM distributions in all these structures follow the same scaling relation allows to conjecture that the observed scaling is a “baryon-independent” characteristics of DM halos.

A strong argument in favor of such a conjecture is given by agreement of the relation (2) derived from observational data with a similar relation derived from *pure DM* N-body simulations, performed in the framework of the Λ CDM model [13]. The distributions of DM particles in simulated halos are fitted by a density profile, from which \mathcal{S} is computed using Eq. (1). As discussed in [9], not only the trend $\mathcal{S} \sim M^{0.2}$, but also the scatter of individual objects around the average (the pink shaded region in the Fig. 1 represents 3σ scatter of the data from the simulations of Ref. [13]) and a different slope for dwarf satellite galaxies (gray dashed line) are reproduced extremely well. The quantity \mathcal{S} is computed using the best-fit models obtained by different groups of observers for each object and compared directly with the results of numerical simulations, without questioning the suggested values of M and \mathcal{S} . The agreement with N-body simulations confirms that, despite different nature and quality of the observational data, the relation 2 is a physical effect rather than a consequence of an observational bias. Our goal here is to explain this property of the Λ CDM model.

Secondary infall model. In spite of apparent simplicity of relation (2) no qualitative explanation and/or analytical derivation of the observed decrease of the average halo density with the increase of the halo mass or size has been proposed so far. In what follows we show that this effect could be readily understood within a semianalytical model of structure formation, known as “secondary infall” model. Within this model, the column density \mathcal{S} is expected to change slowly with the increase of the overall halo mass, $\mathcal{S} \sim M_{\text{halo}}^\kappa$, with $\kappa \leq 1/3$. Under some simplifying assumptions (see below), the upper limit $\kappa = 1/3$ is achieved in structures which continue to grow at present.

The secondary infall model [15–20] (see also [21] for a recent review) provides an analytic description of the growth of the mass $M(t)$ and size $R(t)$ of DM halos in the course of spherically symmetric accretion from cosmological matter flow. One assumes that initial overdensity at the time t_i is distributed in a spherically symmetric way so that the initial mass distribution depends only on the distance r from the inhomogeneity center

$$m(r, t_i) = \frac{4\pi}{3} \rho_M(t_i) r^3 + \delta m_i(r) \quad (3)$$

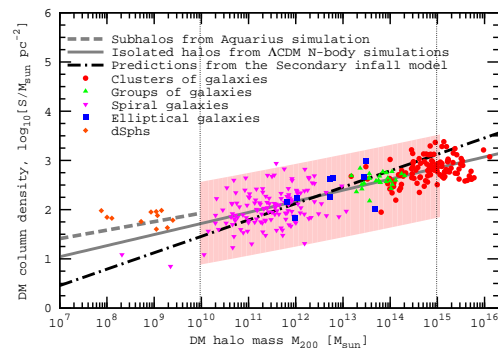


FIG. 1: Column density \mathcal{S} as a function of halo mass M_{200} . The gray solid line is the relation (2), coinciding with predictions of N-body simulations [13], using the WMAP5 [2] cosmological parameters. The shaded region shows the 3σ scatter in the simulation data. The vertical lines indicate the mass range probed by simulations. The gray dashed line shows the results of the Aquarius simulation [14] for sub-haloes. The black dashed-dotted line follows from the infall model.

where $\rho_M(t_i) = (6\pi G t_i^2)^{-1}$ is the cosmological matter density and $\delta m(r)$ is distance-dependent mass excess.¹

The entire DM distribution is split into thin shells parameterized by their initial radii $r_i = r(t_i)$. Evolution of the radius $r(t)$ of each shell is governed by the Newtonian dynamics

$$\frac{d^2 r}{dt^2} = -\frac{\partial U(r)}{\partial r} = -\frac{Gm(t)}{r^2}, \quad (4)$$

where $U(r)$ is the gravitational potential and $m(t)$ is the mass inside the radius $r(t)$. Initial velocities of the shells are assumed to follow Hubble law $\dot{r}(t_i) = H(t_i)r_i$, with $H(t)$ being the expansion rate of the Universe.

If $\delta m_i(r_i) > 0$ expansion of the shell with given r_i slows down faster than it would do in the absence of central overdensity. A straightforward calculation allows to find the time t_* at which $\dot{r}(t_*) = 0$ and the shell reaches maximum (turnaround) radius $R_* = r(t_*)$

$$t_* = \left(\frac{\pi^2 R_*^3}{8Gm_i} \right)^{1/2}; \quad R_* = r_i \frac{m_i}{\delta m_i(r_i)}. \quad (5)$$

At any given moment of time t one can define the boundary of the spherical halo $R(t)$ as the turnaround radius of a shell for which $t = t_*$. From Eq.(5) the mass within this radius, $M(t) = m_i$, is related to $R(t)$ via

$$R(t) = \left(\frac{8GM(t)t^2}{\pi^2} \right)^{1/3}. \quad (6)$$

Continuous growth of the size and mass of the spherical halos is similar to spherically symmetric accretion onto a central

¹ We neglect Λ -term for sufficiently early t_i .

mass concentration. In the accretion theory, the “sphere of influence” of a body with the mass M is defined as the distance range within which the gravitational potential $U = GM/R$ is larger than the specific kinetic energies of accreting particles. In cosmological settings, the given kinetic energy of particles is that of the Hubble flow, $K = (H(t)R)^2/2$. For each R it decreases with time. This leads to the continuous increase of the sphere of influence of the halo with the mass M : $R \propto M^{1/3}/H^{2/3}$ and, respectively, to the growth of the halo mass M , as Eq. (6) demonstrates. The accretion from the cosmological flow could stop if the “sphere of influence” of a given DM halo starts to intersect with the “spheres of influence” of the neighboring halos.

At late stages of evolution of the Universe, the rate of accretion onto a DM halo could diminish due to the influence of the cosmological constant onto the dynamics of cosmological expansion in the direct vicinity of the halo. Modification of the gravitational potential entering Eq. (4)

$$U(r) = -\frac{GM}{r} - \frac{4\pi G\rho_\Lambda}{3}r^2 \quad (7)$$

by a cosmological constant (with the energy density ρ_Λ) leads to a modification of the relation (5) between the R_* and t_* to

$$t_* = \left(\frac{\pi^2 R_*^3}{8GM}\right)^{1/2} f(\lambda) \quad ; \quad \lambda = 4\pi\rho_\Lambda R_*^3/(3M) \quad (8)$$

where $f(\lambda) \equiv (2/\pi) \int_0^1 dx/\sqrt{(x^{-1}-1) + \lambda(x^2-1)}$. For the fixed t_* , the relation (8) has the form $\lambda^{1/2}f(\lambda) = \text{const}$. This means that, for the fixed t_* , $\lambda = \text{const}$ and, therefore, the relation between R_* and M , implied by (6), still holds, although with $\approx 20\%$ different normalization.

Once the shell passes the turnaround radius, it starts to oscillate around the center of the halo. The shell will cross other shells and its dynamics will become dependent on their movement. The amplitude of oscillations decreases with time, as long as accretion from the cosmological matter flow continues. The average (over the shells) radial density profile of the halo changes with time. In general, no analytic solution could be found for the dynamics of each shell and the average halo density profile. However, the study of the halo growth simplifies if one considers initial perturbations with power-law profiles

$$\frac{\delta M_i}{M_i} = \left(\frac{M_0}{M_i}\right)^\epsilon, \quad (9)$$

where ϵ is the power-law index and M_0 is a normalization constant (see [19, Sec III.D] for the discussion of the relation of the value of ϵ and initial spectrum of density perturbations). In this case the halo density profile evolves in a “self-similar” manner: its shape can be expressed as

$$\rho(r, t) = \frac{M(t)}{R^3(t)} \times F\left(\frac{r}{R(t)}\right). \quad (10)$$

The function $F(x)$ is the “self-similar” (time and mass scale independent) DM radial density profile with a characteristic

radius x_C . Self-similar solutions exist also in a more general infall models, considered in [19]. One can introduce for each shell an angular momentum ℓ , while still keeping the problem spherically symmetric [19]. If the angular momentum $\ell = jR_*^2/t_*$ with $j = \text{const}$, the initial conditions (9) still lead to a self-similar solution. The detailed shape of the function $F(x)$ can be found numerically. Its asymptotic behavior is given by [19]

$$F(x) \propto \begin{cases} x^{-\gamma}, & x \ll x_C, \quad \gamma = \frac{9\epsilon}{3\epsilon + 1} \\ x^{-2}, & x \gg x_C \end{cases} \quad (11)$$

The property of self-similarity allows to derive the behavior of the column density $\mathcal{S} \propto \bar{\rho}_C r_C = \bar{\rho}_C x_C R(t)$ as a function of M :

$$\mathcal{S} \propto \frac{M(t)}{R^2(t)} x_C \propto M^{1/3}(t) t^{-4/3} \quad (12)$$

where in the second relation we use the Eq. (6) and $x_C = \text{const}$.

Equation (12) expresses the universal scaling relation between halo column density and mass. It is a direct analog of relation (2) within the secondary infall model. Notice, that it provides an explanation, at least at the qualitative level, of the observed *slow* growth of the DM column density with the increase of the halo mass. At the same time, the Eq. (12) contains, apart from the mass M , an additional parameter t , the time during which the halo accretes from the cosmological matter flow.

Notice that Eq. (6) (or its analog (8)) implies that all structures which accrete up to the time t have the same average density $\rho_R(t) = M(t)/[(4\pi/3)R^3(t)]$ equal to $\text{const} \times \rho_M(t)$ (the cosmological density at the time t). For cosmologically close objects (including those, analyzed in [9]) accretion still continues, i.e. $t = t_0$ (the present age of the Universe). If accretion onto a halo has terminated at time $t_{\text{final}} < t_0$, (this is the case, for example, for the dwarf spheroidal satellites of the Milky Way), then according to relation (12) the DM column density of such objects will be higher for the same mass.

For the density profile of the form (10, 11) the DM column density (1) is given by

$$\mathcal{S} = \frac{\alpha}{x_C} \left(\frac{\pi^2}{8G}\right)^{2/3} \frac{M^{1/3}(t_{\text{final}})}{t_{\text{final}}^{4/3}}, \quad (13)$$

where α is a numerical coefficient which could be found from numerically calculated profiles $F(x)$. Choosing a typical value for $x_C \sim 0.02$ [19], one obtains $\mathcal{S} = 133M_\odot/\text{pc}^2$ for $M \simeq 10^{12}M_\odot$. The relation (13) (for $M = M_{200}$) with this normalization is shown by the dashed-dotted line in Fig. 1.

Discussion. The universal scaling relation between the mass and column density of DM halos (12), derived within the simple semianalytical model of self-similar secondary infall provides a reasonable description of the data presented in

Fig. 1. The scaling $\mathcal{S} \sim M^{1/3}$ is determined mostly by two properties of the model: (i) Average density inside the sphere of the radius $R(t)$ is the same for all DM halos, independently of their mass. It is equal, up to a constant, to the cosmological matter density at the moment t , see Eq. (6) and (8). (ii) Radial density profiles of all halos are approximately the same (the self-similarity condition (10)), independently of their mass.

The statement (i) is just a general consequence of the physics of accretion from cosmological matter flow. The self-similarity property (ii) is a simplifying assumption. Although it is present in the simplest solutions of the infall model (see [19]) and the data suggest that the deviation from the self-similarity are not so big, it may or may not hold in realistic structure formation. Validity of this assumption could be verified via comparison with N-body simulations of structure formation. In the simulations, density profiles of halos are usually fitted by two-parametric NFW profiles, which may be characterized, for example, by the scales $r_C = r_s$ and R_{200} . The NFW profiles which arise in the simulations are known (see e.g. [13]) to satisfy the relation

$$c_{200} \propto M_{200}^{-0.1}, \quad (14)$$

where $c_{200} = R_{200}/r_s \propto 1/x_C$. The dependence of x_C upon mass scale is rather weak and the density profiles predicted by N-body simulations do form, to a good approximation, a self-similar subset of all NFW profiles.

The small deviation from self-similarity, described by the Equation (14), explains a somewhat better fit to the data provided by the N-body simulations. Expressing x_C from Eq. (14) and substituting it into (13) one finds $\mathcal{S} \sim M^{0.23}$, rather than $\mathcal{S} \sim M^{1/3}$, which is closer to the $\mathcal{S}(M)$ scaling relation (2) derived from the observational data.

In the frameworks of the infall models deviations from self-similarity arise from slight dependence of ϵ in initial conditions (9) and/or the angular momentum ℓ on the mass scale [19]. Finally, dependence of the $\mathcal{S}(M)$ scaling (13) on t_{final} introduces additional correction for structures in which $t_{\text{final}} < t_0$. More precise understanding of the deviations from the simplest approximation, discussed above, together with better quality of the data, would allow to observationally constrain the details of cosmological DM halo formation process. The detailed analysis of the small deviations from the self-similar infall model is, however, beyond the scope of the present Letter.

Conclusions. The universal $\mathcal{S}-M$ scaling in the DM halos, found in the observational data and in pure DM N-body simulations can be analytically understood in the secondary infall model. It seems to be insensitive to the presence of baryons and to the details of DM density distributions. This shows that this relation has pure DM origin (in contrast with its interpretation in favor of Modified Newtonian Dynamics, as discussed e.g. in [8]).

Qualitative understanding of the scaling between the den-

sity and size of DM halos discussed in this Letter, opens a possibility to estimate expected modification of the scaling over a broad parameter space of alternative models of DM (such as e.g. [3]) and/or large-scale modifications of gravity (see [22]) and, therefore, distinguish between different classes of such models. In this respect, the simplified analytical approach of the secondary infall model provides a valuable alternative to resource consuming N-body simulations.

The predictions of the secondary infall model can be tested in the Local Group [20], using e.g. the data on the local Hubble flow [23]. Our results also motivate dedicated astronomical search, especially for the isolated galaxies with the masses below $10^{10}M_\odot$ (two pink downward triangles in Fig. 1) and systematic studies of DM content in galaxy clusters, as well as a uniform analysis of all observations collected in [9]. This would allow to reduce systematic errors in the data, determine more precisely the slope in relation (2) and find possible deviations from the pure CDM model.

This work was supported in part by the SCOPES project No. IZ73Z0_128040 and by the Swiss National Science Foundation.

-
- [1] L. Bergstrom, *New J. Phys.* **11**, 105006 (2009).
 - [2] E. Komatsu et al., *Astrophys. J. Suppl.* **180**, 330 (2009).
 - [3] P. Bode, J. P. Ostriker, and N. Turok, *ApJ* **556**, 93 (2001).
 - [4] G. R. Dvali, G. Gabadadze, and M. Porrati, *Phys. Lett.* **B485**, 208 (2000).
 - [5] M. Milgrom, *Astrophys. J.* **270**, 365 (1983).
 - [6] J. Kormendy and K. C. Freeman, in *Dark Matter in Galaxies*, edited by S. Ryder, D. Pisano, M. Walker, & K. Freeman (2004), vol. 220 of *IAU Symposium*, p. 377, CUP
 - [7] F. Donato et al., *MNRAS* **397**, 1169 (2009).
 - [8] G. Gentile, B. Famaey, H. Zhao, and P. Salucci, *Nature* **461**, 627 (2009).
 - [9] A. Boyarsky et al., 0911.1774 (2009).
 - [10] J. F. Navarro, C. S. Frenk, and S. D. M. White, *ApJ* **490**, 493 (1997).
 - [11] A. Burkert, *ApJ* **447**, L25+ (1995).
 - [12] A. Boyarsky et al., *Phys. Rev. Lett.* **97**, 261302 (2006).
 - [13] A. V. Macciò, A. A. Dutton, and F. C. van den Bosch, *MNRAS* **391**, 1940 (2008).
 - [14] V. Springel et al., *MNRAS* **391**, 1685 (2008).
 - [15] J. E. Gunn and J. R. I. Gott, *ApJ* **176**, 1 (1972).
 - [16] J. A. Fillmore and P. Goldreich, *Astrophys. J.* **281**, 1 (1984).
 - [17] E. Bertschinger, *Astrophys. J. Suppl.* **58**, 39 (1985).
 - [18] P. Sikivie, I. I. Tkachev, and Y. Wang, *Phys. Rev. Lett.* **75**, 2911 (1995).
 - [19] P. Sikivie, I. I. Tkachev, and Y. Wang, *Phys. Rev.* **D56**, 1863 (1997).
 - [20] G. Steigman and I. Tkachev, *ApJ* **522**, 793 (1999).
 - [21] A. Del Popolo, *Astrophys. J.* **698**, 2093 (2009).
 - [22] A. Boyarsky and O. Ruchayskiy, 1001.0565 (2010).
 - [23] I. D. Karachentsev, O. G. Kashibadze, D. I. Makarov, and R. B. Tully, *MNRAS* **393**, 1265 (2009).